TISSUE ENGINEERING: Part A
Volume 14, Number 7, 2008

DOI: 10.1089/ten.tea.2007.0225

Optimization of Allograft Implantation Using Scaffold-Free Chondrocyte Plates

TOSHIHIRO NAGAI, M.D.,[1] MASATO SATO, M.D., Ph.D.,[1] KATSUKO S. FURUKAWA, Ph.D.,[2] TOSHIHARU KUTSUNA, M.D.,[1] NAOSHI OHTA, M.D.,[1] TAKASHI USHIDA, Ph.D.,[3] and JOJI MOCHIDA, M.D., Ph.D.[1]

ABSTRACT

If a tissue-engineered cartilage transplant is to succeed, it needs to integrate with the host tissue, to endure physiological loading, and to acquire the phenotype of the articular cartilage. Although there are many reported treatments for osteochondral defects of articular cartilage, problems remain with the use of artificial matrices (scaffolds) and the stage of implantation. We constructed scaffold-free three-dimensional tissue-engineered cartilage allografts using a rotational culture system and investigated the optimal stage of implantation and repair of the remodeling site. We evaluated the amounts of extracellular matrix and gene expression levels in scaffold-free constructs and transplanted the constructs for osteochondral defects using a rabbit model. Allografted 2-week constructs expressed high levels of proteoglycan and collagen per DNA content, integrated with the host cartilage successfully, and were able to counter physiological loads, and the chondrocyte plate contributed reparative mesenchymal stem cells to the final phenotype of the articular cartilage.

INTRODUCTION

MATURE ARTICULAR CARTILAGE has a limited capacity for regeneration after degeneration or injury.[1] However, none of the methods currently used to repair damaged cartilage can restore a durable articular surface to an osteoarthritic joint predictably.[2] Recently, three-dimensional (3D) tissue-engineered cartilage has been investigated intensively, using varieties of artificial matrices and bioreactors.[3] Scaffolds provide a 3D structure and help control the shape of the regenerated cartilage for implantation. However, they can present problems with cell distribution, attachment, proliferation, and biocompatibility, and these drawbacks pose ongoing challenges.

A successful approach to tissue-engineered cartilage must provide for construct survival, providing mechanical stability and permitting integration with the adjacent host tissue after implantation. An *in vitro* study showed better integration between native and engineered cartilage using constructs at an earlier rather than a later stage of chondrogenesis.[4] Thus, biochemical and biomechanical assays were the criteria for assessing tissue maturity and the timing of implantation. Moreover, successful regeneration of any tissue requires the presence of reparative cells with the potential to differentiate into the phenotypes required to restore the damaged site, but it must also provide a microenvironment that supports the proliferation and differentiation of those cells.[5,6]

[1]Department of Orthopedic Surgery and Surgical Science, School of Medicine, Tokai University, Kanagawa, Japan.
[2]Department of Bioengineering and Department of Mechanical Engineering, School of Engineering, University of Tokyo, Tokyo, Japan.
[3]Division of Biomedical Material and Systems Center for Disease Biology and Integrative Medicine, Faculty of Medicine, University of Tokyo, Tokyo, Japan.

We have reported that chondrocytes can be harvested as sheets and made into multilayered tissue allografts to repair a rabbit model with partial-thickness defects in articular cartilage using temperature-responsive culture dishes.[7] Such scaffold-free cell sheets might protect the tissue from proinflammatory agents present in the synovial fluid during experimental implantation. Recently, we constructed 3D, scaffold-free, tissue-engineered cartilage to act as cores for treating total-thickness defects. These constructs induced cell aggregation and eventually formed 3D chondrocyte plates. We used rotational culture to induce an appropriate shearing stress.

The objectives of this study were to conduct a histological, biochemical, and gene expression analysis of the scaffold-free chondrocyte plate and to evaluate whether a chondrocyte plate could integrate with total-thickness defects in the knee joints of rabbits. We also aimed to describe the course of differentiation of host mesenchymal stem cells (MSCs) derived from the bone marrow, comparing plate insertion and control noninsertion groups at early stages of implantation.

MATERIALS AND METHODS

Animal experiments were approved and carried out following the guidelines on animal use of Tokai University and Tokyo University.

Isolation of chondrocytes

Articular cartilage slices from the knee and shoulder joints were obtained from 4-week-old male Japanese white rabbits weighing approximately 1 kg. Slices were minced and digested in Dulbecco's modified Eagle medium (DMEM)/F12 (Gibco, Invitrogen Corporation, Carlsbad, CA) containing 0.4% (w/v) actinase E (Kaken Pharmaceutical Inc., Tokyo, Japan) for 1 h and then in DMEM/F12 containing 0.016% (w/v) bacterial collagenase P (Roche Diagnostics GmbH, Mannheim, Germany) for 3 h. The digested tissue was passed through a cell strainer (Becton Dickinson Labware Co. Ltd, Franklin Lakes, NJ) with a pore size of 70 μm. The filtered material was centrifuged at $200\times g$ for 5 min to separate the cells. The washed pellet was resuspended in medium consisting of DMEM/F12, 10% fetal bovine serum (Gibco), 100 U/mL penicillin (Gibco), 100 μg/mL streptomycin (Gibco), 0.25 μg/mL Fungizone (Gibco), and 50 μg/mL ascorbic acid (Wako Pure Chemical Industries, Ltd, Osaka, Japan). Chondrocytes were seeded on 500 cm^2 square dishes at 1×10^4 cells/cm^2 at 37°C in an atmosphere of 5% carbon dioxide (CO_2) in air and 95% humidity. After approximately 1 week, primary passage cells were detached using 0.05% trypsin/ethylenediaminetetraacetic acid (EDTA; Gibco) for 20 to 30 min at 37°C. The cells were centrifuged as above, washed three times, and then counted in a hemocytometer. The cells were resuspended in medium and then placed into square dishes at a concentration of 1×10^4 cells/cm^2 for two passages.

Scaffold-free tissue-engineered cartilage: chondrocyte plate

We harvested chondrocytes after second passages in monolayer cultures. High-density suspensions of second-passage cells were adjusted to 1.0×10^7 cells/mL in DMEM/F12 supplemented with 20% fetal bovine serum, 100 U/mL penicillin, 100 μg/mL streptomycin, 0.25 μg/mL Fungizone, and 50 μg/mL ascorbic acid. Cylindrical molds (diameter, 10 mm; height, 10 mm; Iwaki, Tokyo, Japan) with a pore size of 0.4 μm were then put on each culture insert (Corning Coastar Japan, Tokyo, Japan). Six hundred microliters of the cell suspension (6×10^6 cells) was inoculated in the mold (Fig. 1A). The cell suspension in the mold showed cell aggregation by 8 h, producing a chondrocyte plate. The mold was then removed (Fig. 1B). In a preliminary experiment, the shape of the chondrocyte plate changed, undergoing deformity or contraction after rotational culture if the primary static culture had been maintained for less than 4 days. Then the plate was cultivated in primary static culture for 7 days until it formed a regular cylindrical shape under dynamic culture conditions. It was then moved into a six-well dish using a medicine spoon and subjected to rotational culture using an orbital shaker (Fig. 1C). The construct was rotated at 70 revolutions/min (rpm) for 3 weeks in a humidified 5% CO_2 incubator at 37°C. The orbital shaker rotates horizontally with a radius of gyration of 25 mm. The culture medium was replaced completely every 2 to 3 days.

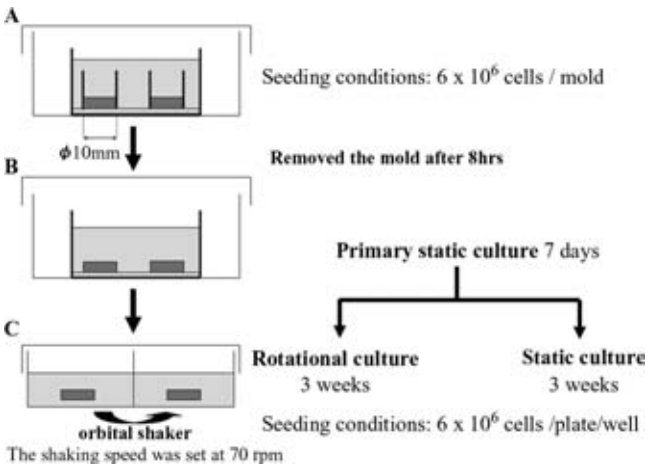

FIG. 1 Construction of the chondrocyte plate. (**A**) The cell suspension was inoculated in the mold. (**B**) After 8 h, the chondrocyte plate had formed, and the mold was removed. The chondrocyte plate was cultured under primary static culture for 7 days. (**C**) The constructs were moved onto nonadherent dishes, which were then cultured under rotational culture or static culture conditions for 3 weeks.

Biochemical analyses

The chondrocyte plates and normal articular cartilage (NAC) of 4-week-old Japanese white rabbits were used for biochemical analyses (five constructs duplicated from four different rabbits per group). Samples were frozen, lyophilized and digested with 1000 μL aliquots of papain (Sigma-Aldrich Co., St Louis, MO) at 125 μg/mL in 0.1 M sodium phosphate with 5 mM Na_2-EDTA and 5 mM cysteine–hydrochloric acid (HCl) at pH 6.0, and incubated at 60°C for 15 h. DNA content was measured spectrofluorometrically using 4,6-diamidino-2-phenylindole, with purified calf thymus DNA as a standard. The glycosaminoglycan content in each chondrocyte plate was determined spectrophotometrically using the dimethylmethylene blue method[8] and shark chondroitin sulfate as a standard. Total collagen content in the plate was determined from the hydroxyproline concentration after alkaline hydrolysis and reaction with chloramine T and *p*-dimethylaminobenzaldehyde.[9] The collagen content was calculated using a hydroxyproline-to-collagen ratio of 1:10.[10]

Real-time reverse transcription polymerase chain reaction

The frozen constructs were pulverized using a CRYO-PRESS (Microtec Nition, Chiba, Japan) on liquid nitrogen. Total RNA was isolated using the SV Total RNA Isolation System (Promega Corp., Madison, WI), following the manufacturer's instructions. Absorbances at 260 and 280 nm were measured for RNA quantification and quality control. Each RNA sample was then reverse-transcribed to cDNA using TaqMan RT reagents (Applied Biosystems, Foster City, CA). Using cDNA, polymerase chain reaction (PCR) assays were carried out with primers and probes for connective tissue matrix-specific genes using an ABI SDS 7300 (Applied Biosystems) programmed to run at 40 cycles under standard thermal conditions. An index mRNA level was assessed using a threshold cycle (C_T) value. To control for variability in amplification caused by differences in starting mRNA concentrations, 18S ribosomal RNA was used as an internal standard (Applied Biosystems). The primers were from Invitrogen, and labeled TaqMan probes were from Sigma-Aldrich. Real-time PCR was carried out using TaqMan Universal PCR Master Mix (Applied Biosystems), 900 nM primers (forward and reverse), 250 nM TaqMan probe, and 2 μL of cDNA sample in a total volume of 25 μL. The relative expression of target mRNA was computed from the target C_T values and the 18S C_T value. Chondrocyte plates of primary static culture at 7 days were used as a reference for comparison of the extent of gene expression in the constructs. The relative mRNA levels for each condition were determined by performing quantitative reverse transcription (RT)-PCR three times for each of the five independent constructs. Primers and probes were designed using Primer Express 3.0 (Applied Biosystems), based on sequences from the GenBank database (http://www.ncbi.nlm.nih.gov/GenBank/index.html). The sequences of primers and probes are shown in Table 1.

Preliminary in vivo *implantation*

As an implantation chondrocyte plate, we selected plates with high levels of proteoglycan (PG)/DNA and collagen/DNA or those showing high levels of chondrogenic gene expression. We transplanted both kinds of plates for preliminary experiments.

In vivo *implantation*

Ten Japanese white rabbits (female, 16–18 weeks old, weighing ~3 kg) were used in this study. The rabbits were anesthetized with intramuscular injections of 120 mg ketamine and 9 mg xylazine. After a medial parapatellar incision to both legs, each patella was dislocated laterally, and a superficial osteochondral defect (5 mm in diameter and 3 mm deep) was created on the patellar groove of the femur in both legs using a drill and a biopsy punch (Kai Industries Co., Seki City, Japan). The bottom of the subchondral bone was shaved to a plane using a biopsy punch until bleeding

Table 1. List of Primers Used in Real-time Reverse Transcriptase Polymerase Chain Reaction

Primer and Probe	*Accession No.*	*Sequence*	*Expect size (bp)*
Collagen type I-F	D49399	GCC TCG CTC ACC ACC TTCT	77
Collagen type I-R		CAA TCT GGT TGT TCA GAG ACT TCA G	
Collagen type I-Probe		CAG ACC CAA GGA CTA TGA AGT CGA TGC C	
Collagen type II-F	D83228	GCA GCA CGT GTG GTT TGG	67
Collagen type II-R		CAG GCT GCT GTC TCC ATA GCT	
Collagen type II-Probe		AGA CCA TCA ATG GCG GCT TCC ACT T	
Collagen type X-F	AF247705	AAC CTG GAC AAC AGG GAC TTA CA	100
Collagen type X-R		TCC CCT TTC TGT CCA CTC ACA	
Collagen type X-Probe		CCC CCG CGG CTT TCC TGG	

TaqMan probes were labeled with the reporter dye molecule 6-carboxyfluorescein at the 5′ end with quencher dye 6-carboxy-*N,N,N′,N′*-tetramethylrhodamine at the 3′ end.

was seen from the marrow. The rabbits were classified into two recipient groups: a chondrocyte plate insertion group, in which the plates were allografted into the created defect, and a noninsertion control group. Before allograft transplantation, the chondrocyte plates were adjusted to the size of the defects using a biopsy punch. The chondrocyte plates were inserted into the defects so that each construct's surface was flush with the host articular cartilage and then left without any additional fixation. The chondrocyte plate filled only the upper part of the lesion, not the entire 3-mm-deep defect. After recovery from the surgery, all animals were allowed to walk freely in their cages without any splints.

Histological evaluations in vitro *and* in vivo

The rabbits were sacrificed 1 month after the operation using an overdose of intravenous anesthetic. The distal part of the femur was excised and fixed with 4% paraformaldehyde for 7 days. Each specimen was decalcified in a solution of 10% EDTA in distilled water (pH 7.4) for 2 to 3 weeks and then embedded in paraffin wax and sectioned perpendicularly (4.5-μm sections) through the center of the defect. Each section was stained with safranin O for glycosaminoglycans and with Masson's trichrome. The chondrocyte plates were also fixed in 4% paraformaldehyde for 7 days, embedded in paraffin wax, and sectioned (4-μm sections).

Immunohistochemistry was done as described.[11] Briefly, sections were deparaffinized according to standard procedures. The sections were treated with 0.005% proteinase (type XXIV, Sigma-Aldrich) for 30 min at 37°C for antigen retrieval. For types I and II collagen, a primary mouse monoclonal antibody (Daiichi Fine Chemical Co., Toyama, Japan) diluted 1:200 in phosphate buffered saline (PBS) + 1% bovine serum albumin (BSA; Sigma-Aldrich) (final concentration 2.5 μg/mL) was placed on the section overnight at 4°C. For chondromodulin-I (ChM-I), a primary goat polyclonal antibody (Santa Cruz Biotechnology, Inc., Santa Cruz, CA) diluted 1:200 in PBS + 1% BSA (final concentration 1 μg/mL) was placed on the section overnight at 4°C. For vascular endothelial growth factor (VEGF), a primary mouse monoclonal antibody (Upstate, Lake Placid, NY) diluted 1:50 in PBS + 1% BSA (final concentration 20 μg/mL) was placed on the section overnight at 4°C. The slides were washed with PBS after incubation for 1 h at room temperature with biotin-conjugated goat antimouse secondary antibody for type I collagen, type II collagen, and VEGF and with biotin-conjugated donkey antigoat secondary antibody for ChM-I. The slides were then treated with horseradish peroxidase–labeled streptavidin for 1 h. They were then soaked in a 0.05% solution of diaminobenzidine in Tris-HCl buffer (pH 7.6) containing 0.005% hydrogen peroxide. Slides were counterstained with Mayer's hematoxylin.

Scanning electron microscopy

The samples were fixed in 2.5% glutaraldehyde (TAAB, Berkshire, UK)/0.1 M phosphate buffer (pH 7.2) at 4°C for 6 h and postfixed in 1% osmic acid/0.1 M phosphate buffer at 4°C for 2 h. They were then dehydrated in a graded ethanol series (50%, 70%, 80%, 90%, and 100%). The samples were immersed in *t*-butyl alcohol (Wako) and frozen at − 20°C. They were freeze-dried using the Inoue and Osatake method,[12] spatter-coated with gold (JFC-1100E JEOL, Tokyo, Japan), and then observed using scanning electron microscopy (SEM) (JSM-840, JEOL).

Statistical analysis

Biochemical data were analyzed using one-factor analysis of variance followed by individual *post hoc* comparisons (Tukey/Kramer). $P < 0.05$ was accepted as statistically significant for any differences.

RESULTS

Histology

After 2 weeks of rotational culture, the chondrocyte plates were considered stable enough to be handled with surgical forceps. Each plate had a regular cylindrical shape and the macroscopic appearance of cartilage (Fig. 2A, B). When a cell suspension was inoculated in a mold, cell aggregation was observed 8 h later using SEM (Fig. 2C). After primary static culture for 7 days, a chondrocyte plate formed with a 1- to 2-μm-thick extracellular matrix (ECM), appearing like a honeycomb shaped scaffold (Fig. 2D). Chondrocytes and ECM were distributed uniformly in the plate. The chondrocytes in the central region of the chondrocyte plate were spherical, but those at the top of the plate had lost their spherical shape (Fig. 2F). After 3 weeks of rotational culture, SEM revealed the formation of chondron units, consistent with the native chondrocyte alignment (Fig. 2E). At the same time, the central region of the chondrocyte plate was intensely and uniformly stained with safranin O and was positive for type II collagen. Conversely, the peripheral region of a couple of cell layers in the plate was aligned horizontally to the surface. This zone was not stained with safranin O and was not positive for type II collagen but was positive for type I collagen. This peripheral region formed a capsule around the central region (Fig. 2G–I). Alternatively, after static culture for 4 weeks (primary static culture for 1 week and static culture for 3 weeks), the central region of the chondrocyte plate was irregularly stained with safranin O, positive for type II collagen, but was not positive for type I collagen. Moreover, the peripheral region of the plate was not smooth but opened in pores (Fig. 2J–L).

ECM deposition

The time courses of biochemically analyzed construct components are shown in Figure 3A–E. PG and collagen contents of the constructs increased significantly in rotational

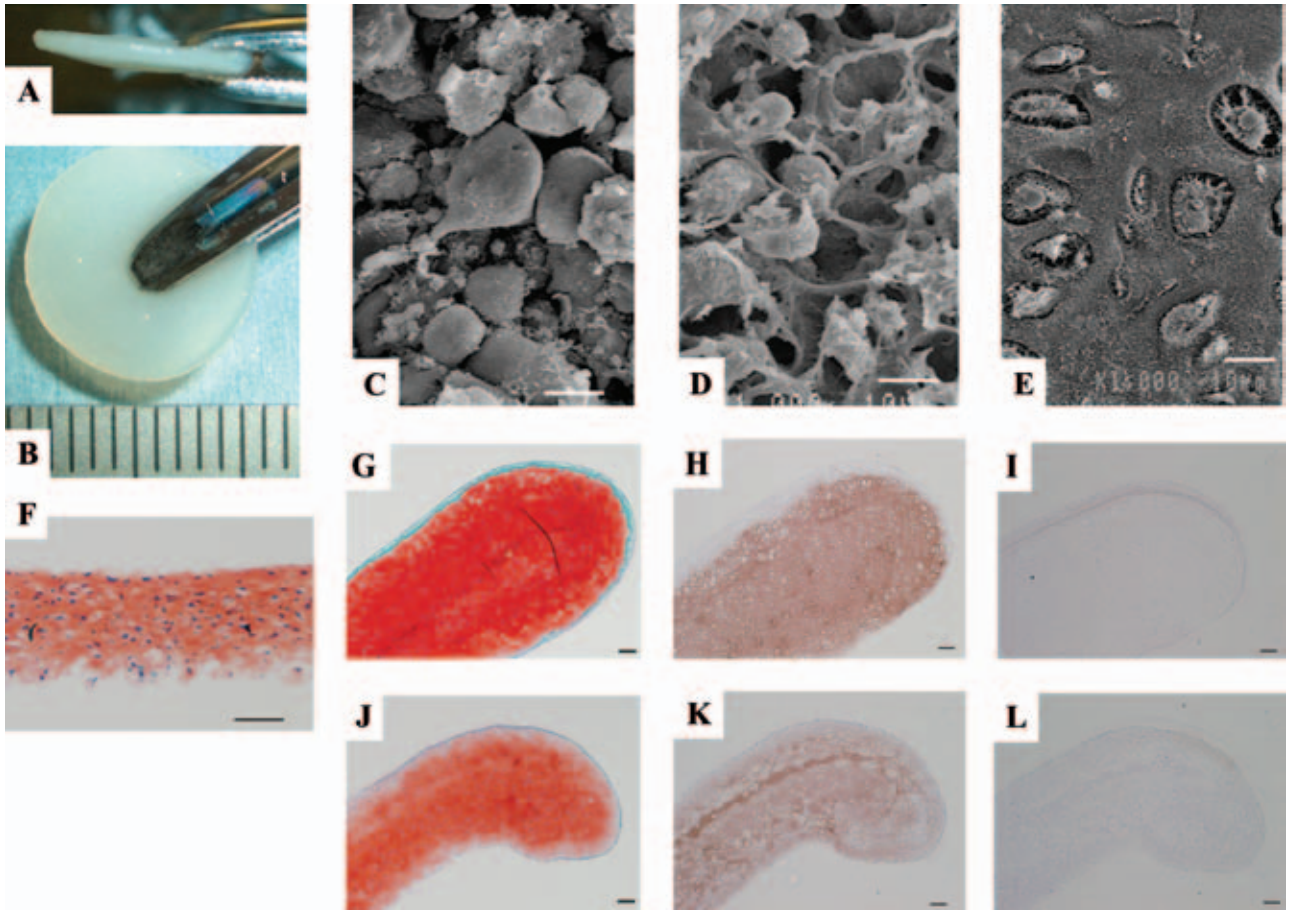

FIG. 2 Macroscopic and histological analyses of the study *in vitro*. (**A, B**) Macroscopically, the chondrocyte plate after 3 weeks of rotational culture resembled cartilaginous tissue (1-mm scale bar below). (**C**) Scanning electron microscopy (SEM) of chondrocyte plates formed after 8 h of inoculation in the mold. (**D**) Chondrocyte plates formed after 7 days of primary static culture. The autologous extracellular matrix (ECM) has a honeycomb appearance. (**E**) Chondrocyte plates formed after 3 weeks of rotational culture. SEM revealed the formation of chondron units. (**F, G, J**) Safranin O staining; (**H, K**) collagen type II immunostaining; (**I, L**) collagen type I immunostaining. (**F**) After primary static culture for 7 days, chondrocyte plates showed an ECM stained uniformly with safranin O. After 3 weeks of rotational culture, (**G**) the central region of chondrocyte plates stained intensely with safranin O and (**H**) was positive for type II collagen. (**I**) The peripheral region of the plates was positive for type I collagen. On the other hand, after 3 weeks of static culture, chondrocyte plates were irregularly and faintly stained with safranin O and were weakly positive for types I and II collagen (scale bars = 1 mm in **B**; 10 μm in **C–E**; 100 μm in **F–L**). Color images available online at www.liebertpub.com/ten.

culture for 3 weeks. By contrast, both reached a plateau after static culture for 2 weeks (Fig. 3A, B). The PG contents in the constructs from the rotational culture were approximately double that of the static culture at 3 weeks, and the collagen contents were approximately 180% of those of the static culture. In the rotational cultures, the DNA content of the constructs increased for 3 weeks, whereas in the static cultures, the DNA content reached a peak in 2 weeks and decreased thereafter (Fig. 3C). PG/DNA of the constructs from the rotational culture increased progressively from primary static culture at 7 days to significantly higher than that of NAC at 2 weeks and then reached a plateau (Fig. 3D). The PG/DNA level of the plates after 2 weeks of rotational culture was 275% of that measured in NAC. However, the collagen/DNA content of the constructs in the rotational culture was significantly higher than in the static culture at 2 weeks. It peaked at this level but was only 47% of that in NAC (Fig. 3E). The collagen/DNA content of NAC was significantly higher than that of the constructs in the rotational and the static cultures through incubation.

Gene expression

The time courses of mRNA level expression of collagen type I, collagen type II, and collagen type X in the constructs from the rotational culture were normalized to those of the constructs in primary static culture at 7 days, as indicated by a value of 1.0 (Fig. 4A–C). Collagen type I mRNA expression increased during the first 2 weeks of rotational culture and decreased thereafter (Fig. 4A). The mRNA expression

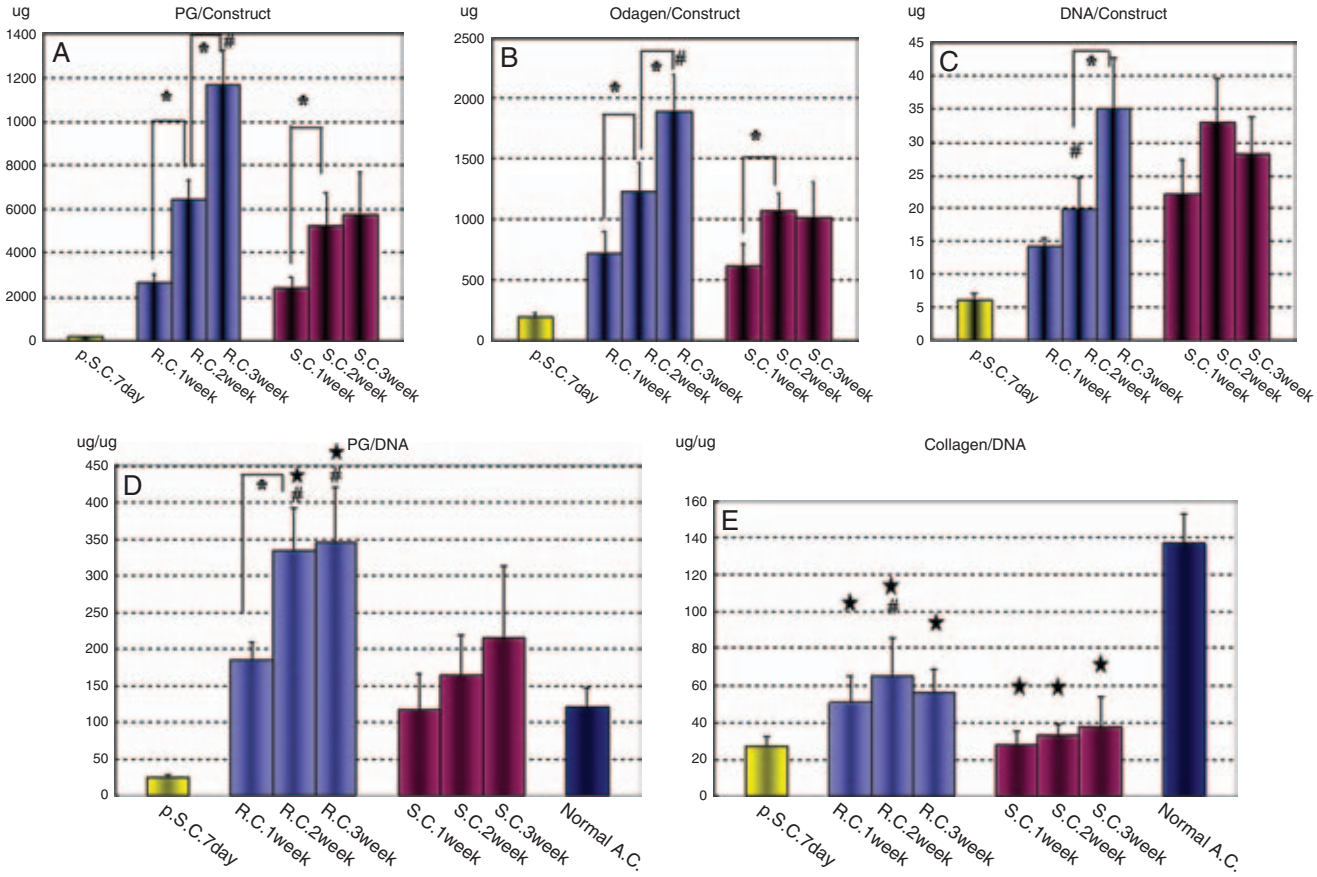

FIG. 3 Quantitative biochemical analyses of proteoglycan, collagen, and DNA contents of the constructs of the chondrocyte plates cultured in primary static culture for 7 days followed by 3 weeks in rotational and static culture conditions. (**A**) Proteoglycan content. (**B**) Collagen content. (**C**) DNA content. (**D**) Proteoglycan DNA. (**E**) Collagen DNA. Values represent the means ± standard deviations of five sets of experiments run in duplicate. $*P < 0.05$ compared with different time points in rotational culture and static culture. $\#P < 0.05$ compared with static culture for the same time. $P < 0.05$, compared with normal articular cartilage. Color images available online at www.liebertpub.com/ten.

of type II collagen of the 1-week chondrocyte plate tended to be high. However, the expression of type II collagen mRNA did not show any significant differences in chondrocyte plates from rotational culture over 1 to 3 weeks (Fig. 4B). The mRNA expression of type X collagen in rotational culture was maintained at the same level as that in primary static culture from 7 days to 2 weeks and increased thereafter (Fig. 4C).

Preliminary in vivo implantation

Messenger RNA expression of type II collagen tended to be high, and type I collagen was still at a low level in the 1-week chondrocyte plates from rotational culture. Alternatively, PG/DNA and collagen/DNA levels were high in the 2-week plates. We transplanted the 1-week and 2-week chondrocyte plates to the total-thickness-defect model. At 4 weeks after implantation, fibrous tissue had replaced most of the 1-week plates, and many inflammatory cells were seen in the subchondral bone (Fig. 5A). Alternatively, 2-week plates maintained their shape and integrated with the host cartilage. In the subsequent studies, we used 2-week chondrocyte plates as grafts (Fig. 5B).

Examination of implanted chondrocyte plates

Operations were uneventful, and all rabbits resumed normal cage activity immediately. All rabbits exhibited an unlimited passive range of knee joint motion at the time they were euthanized.

At 4 weeks after implantation, according to macroscopic observation, the chondrocyte plate insertion group seemed to show better results in terms of the integration of host cartilage, and the defects repaired by the plate were smoother than in the noninsertion group (Fig. 6A, I). In the chondrocyte plate insertion group, the repair site appeared to be filled with cartilaginous tissues, which were strongly stained with safranin O, positive for type II collagen, and negative for type I collagen (Fig. 6B, E, G). Lateral integration of the chondrocyte plate was well bonded at both

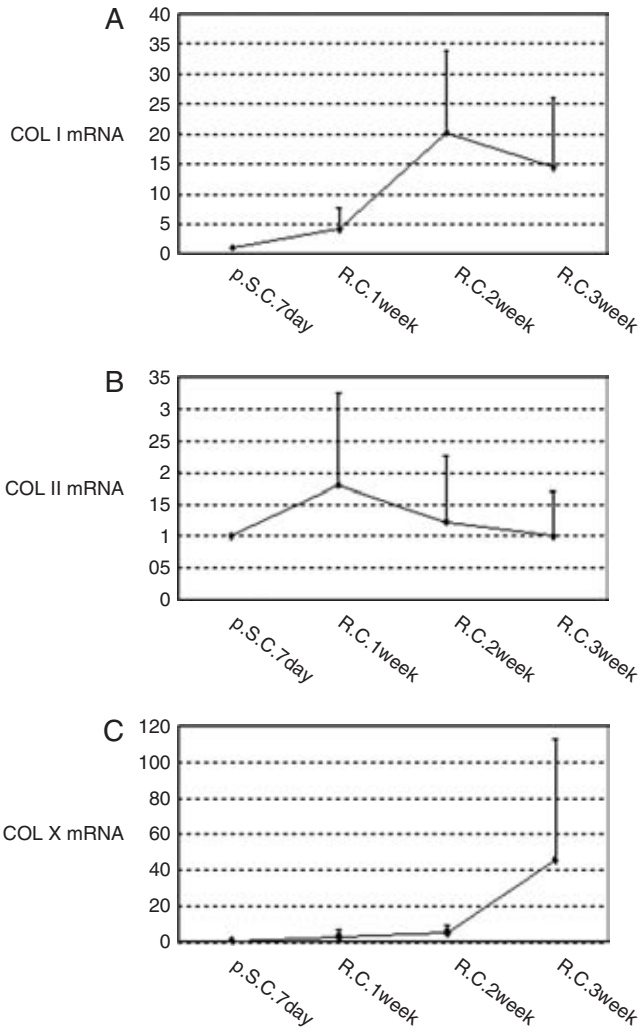

FIG. 4 Gene expression levels using real-time reverse transcription polymerase chain reaction. Gene expression in the chondrocyte plate constructs cultured for up to 3 weeks in primary static or rotational culture conditions. (**A**) The relative gene expression level for type I collagen. (**B**) The relative gene expression level for type II collagen. (**C**) The relative gene expression level for type X collagen. Values represent the means ± standard deviations of five samples with experiments run in duplicates.

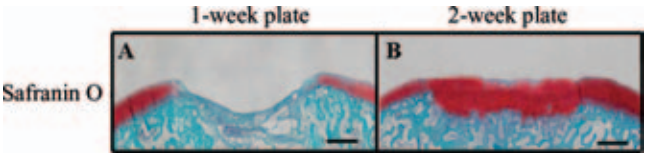

FIG. 5 Preliminary *in vivo* implantation experiments. Histological analyses at 4 weeks (**A**) in the 1-week chondrocyte plate insertion group and (**B**) in the 2-week chondrocyte plate insertion group (scale bars = 1 mm). Color images available online at www.liebertpub.com/ten.

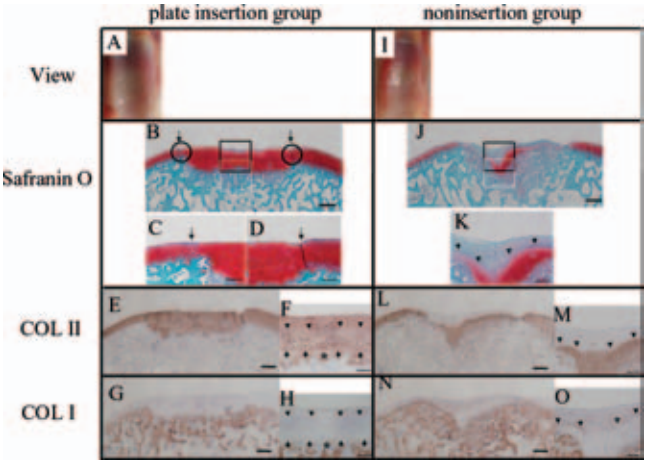

FIG. 6 Macroscopic and histological analyses of the *in vivo* study for safranin O and for types I and II collagen. (**A, I**) Macroscopic observations on femoral condyles at 4 weeks after surgery. (**A**) In the chondrocyte plate insertion group, the defect seemed to be better regarding the integration of host cartilage than in (**I**) the noninsertion control group. (**B–H, J–O**) Histological analyses at 4 weeks. Sagittal sections of the defects were (**B**) stained positively with safranin O and (**E**) were positive for type II collagen and (**G**) type I collagen in the plate insertion group. Sections from the noninsertion group (**J**) were stained with safranin O and were (**L**) positive for type II collagen and (**N**) type I collagen. Higher magnifications of the circle area in (**B**) stained with safranin O (**C and D**); the black-framed area in (**B**), which was positive for (**F**) type II collagen and (**H**) type I collagen. Higher magnifications of the black-framed area in (**J**) stained with (**K**) safranin O and (**M**) positive for type II collagen and (**O**) type I collagen (scale bars = 1 mm in **B, E, G, J, L, and N**; 250 μm in **C, D, F, H, M, and O**). Color images available online at www.liebertpub.com/ten.

sides of host cartilage (Fig. 6C, D). Basal integration of the plate was also good. Each implanted chondrocyte plate was clearly visible but was thinner than before implantation (650–700 μm thick). The interfacial adhesion between the plate and the lower portion of the repair tissue is shown by arrowheads in Figures 6F and H and Figure 7A. The lower portion of the repair tissue contained hypertrophic chondrocytes that were remodeling the subchondral bone. Structural integrity of the plate was shown by the beginning of columnar organization of rounded chondrocytes (Fig. 7B). No infiltration of inflammatory cells within the subchondral bone was seen. Alternatively, in the noninsertion group, the defects were filled with mainly fibrous tissue (Fig. 6J, L, N) concealing the lower portion of the repair tissue. The lower portions of the regions stained with safranin O were positive for type II collagen but not for type I (Fig. 6K, M, O). Black arrowheads indicate the interface between fibrous tissue and the remodeling site of subchondral bone in Figure 6. The interface area was positive for type I collagen. The lower portion of the remodeling site of subchondral bone appeared to be filled with hypertrophic chondrocytes.

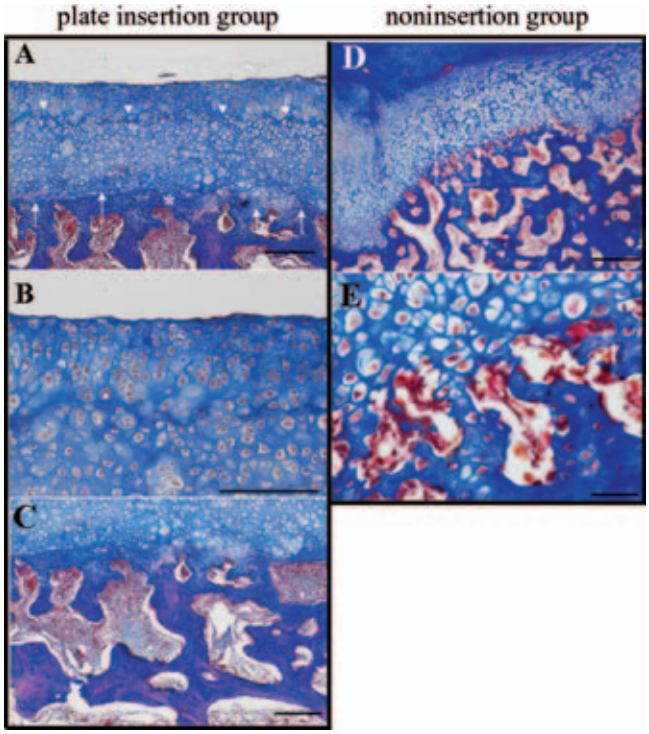

FIG. 7 Histological analyses of the *in vivo* study using Masson's trichrome staining. (**A, B**) Higher magnifications of the black-framed area in Figure 6B. (**C**) Higher magnification of the white-framed area in Figure 6B. (**D**) High magnification of the white-framed area in Figure 6J. (**E**) Higher magnification of the white-framed area in (**D**) stained with Masson's trichrome (scale bars = 250 μm in **A, C, and D**; 200 μm in **B**; 50 μm in **E**). Color images available online at www.liebertpub.com/ten.

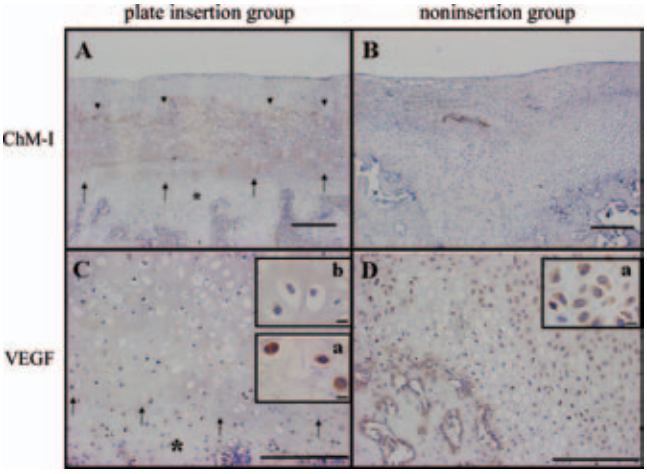

FIG. 8 Histological analyses of the *in vivo* study for chondromodulin-I (ChM-I) and vascular endothelial growth factor (VEGF) expression levels. (**A**) Higher magnification of the black-framed area in Figure 6B, which was positive for ChM-I. (**B**) Higher magnification of the black-framed area in Figure 6J, which was positive for ChM-I. (**C**) Higher magnification of the arrowed area in (**A**), which was positive for VEGF. (**D**) Higher magnification of the white-framed area in Figure 7D, which was positive for VEGF. **C(a)** shows a higher magnification of the asterisked area in (**C**). **C**(**b**) is a higher magnification showing hypertrophic chondrocytes above the arrowed area in (**C**). (**a**) is a higher magnification of hypertrophic chondrocytes in (**D**). (scale bars = 250 μm in **A and B**; 200 μm in **C and D**; 10 μm in **Ca, Cb, and Da**). Color images available online at www.liebertpub.com/ten.

The blood vessels at the bottom of the hypertrophic chondrocyte layer failed to penetrate this zone and were dilated in the plate insertion group (Fig. 7C). Alternatively, in the noninsertion group, the blood vessels penetrated the hypertrophic chondrocyte layer (Fig. 7D, E). In the plate insertion group, ChM-I was intensely positive in the lower portion of the repair tissue, shown between the arrows and arrowheads in Figure 8A. The asterisked area below the arrows was positive for types I and II collagen but not for ChM-I (Fig. 6F, H and Fig. 8A). VEGF was present in the asterisked area (Fig. 8Ca) and was almost absent in the arrowed regions (Fig. 8Cb). In the noninsertion group, no ChM-I was observed in the lower portion of the repair tissue (Fig. 8B). Alternatively, the remodeling hypertrophic chondrocyte layer was intensely positive for VEGF (Fig. 8Da).

DISCUSSION

We consider that the importance of tissue engineering cartilage lies not only in the quantity of ECM that can be produced, but also in maintaining the distribution of the cells and the ECM. Moreover, as a matter of course, the central region of the graft must maintain cartilage differentiation. The distribution of the peripheral region facing in the articular surface is particularly important, because emission of proteoglycan and cellular damage are anticipated if the peripheral region carrying a direct load is not a smooth and tight surface.

In this study, PG/DNA of 2-week plates of rotational culture was 275% of that in NAC, and collagen/DNA of 2-week plates of rotational culture was 47% of NAC. In another study on scaffold-free tissue-engineered cartilage, Grogan *et al.*[13] reported that the dry weight of PG in their neo-cartilage was 83% of NAC and that collagen dry weight was 25% of NAC after 4 weeks culture. Hu *et al.*[14] reported that the PG per dry weight of their constructs formed over agarose was 166% of NAC and that the collagen per dry weight was 33% of NAC after 12 weeks of culture. Park *et al.*[15] reported that the PG content per cell of their scaffold-free constructs was approximately 60% of NAC after 5 weeks of culture. (Collagen content was not assessed.) We were able to construct scaffold-free tissue-engineered cartilage with abundant ECM after a shorter culture period than for other scaffold-free models. The chondrocytes of the peripheral region of the chondrocyte plate in rotational culture were aligned horizontally to the surface. We speculate that our rotational culture system promoted the production of matrices

in the central region and helped develop the peripheral smooth layer.[16,17]

As mentioned above, this is not the first report on scaffold-free tissue-engineered cartilage; similar products have been constructed using rotational wall vessels,[18] using static bioreactor systems,[13,19,20] exploiting the low adhesive property of agarose to cells,[14] and using a specific system.[15] However, the macroscopic and histological appearance of the cartilaginous tissue produced in the latter three approaches had surface irregularities, unlike the smooth cartilaginous tissue surface that we constructed in static culture. Alternatively, the peripheral region of the tissue-engineered cartilage that we constructed in this rotational culture system was smooth and tight. The chondrocytes of the peripheral region lost their rounded shape and were more elongated and oriented parallel to the surface, as is the cartilage surface *in vivo*. We speculate that this smooth surface prevented the loss of aggrecan and the cellular damage caused by loading *in vivo*.

It is important that tissue-engineered cartilage transplants not only provide for construct survival, but also respond to loading adequately after implantation. It is also necessary to determine the optimum implantation stage, but there is no consensus regarding this at present.[2] *In vitro* studies have shown that the integration between native articular cartilage and engineered cartilage is better at an early stage of chondrogenesis than at a later stage.[21] Alternatively, *in vivo,* it is important that arthrodial cartilage be able to endure loads, so a substantial matrix is necessary. Generally, satisfying these conflicting aspects of integration and biomechanical capability is considered to center on the optimal timing of implantation. In this sense, 1-week or 2-week plates from rotational cultivation seem to be optimal, according to the results of gene expression and biochemical analysis. In preliminary experiments, we transplanted plates after rotational culture for 1 week, when chondrogenic gene expression tended to be high. However, fibrous tissue replaced most of the plates, and many inflammatory cells were seen in the subchondral bone (Fig. 5A). Meanwhile, plates in rotational culture for 2 weeks, when PG/DNA and collagen/DNA levels were high, maintained their formation and integrated well with the surrounding host tissues. Hypertrophic chondrocytes from the bone marrow replaced the bottom of the plate, and repairing regions consistently developed matrix composed predominantly of glycosaminoglycans and type II collagen.

Scaffold-free tissue-engineered cartilage must support loads with a self-producing ECM. Therefore, scaffold-free constructs need reliable matrices to endure physiological loading. Park *et al.* implanted 1-week cultures of scaffold-free tissue-engineered cartilage and commented that the implants had collapsed below the nearby cartilage surface.[15] This suggests that the mechanical property of 1-week constructs is inadequate and that the implants are too thin to fill a full-thickness defect. They felt that scaffold-free constructs require more stiffness to counter physiological loads.

In this study, although mRNA expression of type II collagen decreased slightly after 1 week of rotational culture, we selected 2-week rotational culture plates for the verification of implantation *in vitro* and *in vivo*. We considered that PG/DNA and collagen/DNA levels would be a better index of the implantation stage than chondrogenic gene expression in scaffold-free constructs. It is important to evaluate the mechanical properties of tissue-engineered cartilage and to test whether its mechanical properties can bear normal physiological loadings. We did not select 3-week plates because of the high mRNA expression of type X collagen at that time.

Brehm *et al.*[20] investigated superficial osteochondral defects in a caprine model. They commented that superficial osteochondral defects resemble commonly encountered defects in human patients after debridement. These debrided states corresponded closely to the superficial osteochondral defects they created artificially. Therefore, for our model, we assumed that debridement would apply to human patients and created super-osteochondral defects 3 mm deep.

There may be an objection that osteochondral defects in a rabbit model such as we used here might repair spontaneously. In mature rabbits, defects 3 mm in diameter and 2 mm deep are reported to be the critical size for spontaneous repair, and defects of the size we used (5 mm wide, 3 mm deep) do not repair spontaneously.[22]

Host MSC-derived hypertrophic chondrocytes were stained with safranin O and were positive for type II collagen in the plate insertion group and the control noninsertion group (Fig. 6B, E, J, L). ChM-I was found only in the plate insertion group (Fig. 8A). ChM-I staining was intense in the lower portion of the repair tissue containing hypertrophic chondrocytes engaged in remodeling subchondral bone.

Generally, total-thickness defects have access to reparative cells of the bone marrow.[6] This connection allows infiltration of the defect by MSCs from the bone marrow, which can then proliferate and differentiate. MSC-derived hypertrophic chondrocytes appear subsequently during endochondral ossification, and vasculature and marrow, and eventually subchondral bone replace the defects.[5,23] The course of bone remodeling resembles the development of the mammalian embryonic skeleton.[5,24] However, the development of hyaline articular cartilage is not recognized in artificial total-thickness-defect models. By nature, articular cartilage is avascular except during skeletal development, when endochondral bone formation occurs. Capillaries from the surrounding periosteum invade the calcified zone at the center of the previously avascular cartilage shaft. This angiogenesis is thus a pivotal event that coordinates chondrogenesis and subsequent osteogenesis in endochondral bone formation.[25] ChM-I was reported to stimulate chondrocyte proliferation and PG synthesis *in vitro* and to inhibit the proliferation of vascular endothelial cells *in vitro* and *in vivo*.[26,27] Kitahara *et al.*[27] suggested that ChM-I acted to inhibit vascular invasion in the immature state of the articular cartilage and that the levels of ChM-I decreased

gradually with age in the articular cartilage of their mouse model.

In our study, hypertrophic chondrocytes in the noninsertion group produced VEGF (Fig. 8D) but did not show ChM-I (Fig. 8B), and the blood vessels penetrated the hypertrophic chondrocyte layer (Fig. 7D, E). Such vascular invasion promotes the progression of ossification in the total-thickness-defect model. Alternatively, in the plate insertion group, hypertrophic chondrocytes were positive for ChM-I (Fig. 8A) and expressed little VEGF (Fig. 8Cb). Moreover, the blood vessels failed to penetrate the hypertrophic chondrocyte layer (Fig. 7C). This suggests that MSC-derived hypertrophic chondrocytes acquired their antiangiogenic properties from the chondrocyte plate. The levels of ChM-I and VEGF cannot solely account for the modulation of switching from angiogenesis to antiangiogenesis. The presence of inducers of endogenous angiogenic molecules in the process of endochondral ossification has been reported for VEGF,[27] fibroblast growth factor 2 (FGF-2),[28] transforming growth factor beta (TGF-β),[29] and tissue matrix metalloproteinase (MMP)-9.[30] Moreover, there may be the objection that hypertrophic chondrocytes were derived from the allografted chondrocyte plate rather than from the host. We consider that the hypertrophic chondrocyte layer contained donor chondrocytes and host MSC-derived hypertrophic chondrocytes. The 2-week rotational culture chondrocyte plate was 650 to 700 μm thick, and at 4 weeks after implantation, it thinned to approximately 200 μm. Thus, chondrocytes from approximately 450 to 500 μm of the implant were included in the 3-mm-deep defect. Therefore, chondrocytes of the allograft might have hypertrophied. Because we did not label the chondrocyte plate, we could not distinguish between MSC-derived hypertrophic chondrocytes and donor chondrocytes individually. However, in this study, the chondrocyte plate did not fill the entire defect, only the upper part. Moreover, all of the hypertrophic chondrocyte layer (donor chondrocytes and host MSC-derived hypertrophic chondrocytes) in the plate insertion group expressed ChM-I and did not express VEGF. Therefore, we are convinced that the hypertrophic chondrocytes in the defect were derived mainly from host-derived hypertrophic chondrocytes. Thus, at 4 weeks after chondrocyte plate implantation, MSC-derived hypertrophic chondrocytes in the plate insertion group showed lower angiogenesis than in the noninsertion group.

There are limitations in the current methods, and the feasibility of using scaffold-free constructs needs to be verified with mature chondrocytes and even with passaged ones.[15] In preliminary studies, we found that immature rabbit and bovine articular chondrocytes could be used to construct chondrocyte plates after five passages (data not shown). We have also evaluated other cell sources, and this will be published elsewhere.

Here we prepared scaffold-free chondrocyte plates and compared rotational with static culture methods using histological and biochemical analysis. We also evaluated the modulation of gene expression levels of the plates in rotational culture over 1 to 3 weeks. We investigated whether the plates produced by rotational culture, which is considered to provide optimum conditions *in vitro*, integrated with total-thickness defects. Those plates that produced high levels of PG/DNA and collagen/DNA showed satisfactory integration with the surrounding host cartilage and were capable of countering normal loads. The repair site receiving the plate also maintained its cartilaginous matrix. There were differences at the host repair site between the plate insertion group and the noninsertion group at the early stage of implantation. Host MSC-derived hypertrophic chondrocytes produced ChM-I, reduced their production of VEGF, and inhibited angiogenesis in the plate insertion group. Thus, the implantation of the chondrocyte plate altered host MSC-derived hypertrophic chondrocytes to an articular cartilage phenotype. Further investigations are needed to elucidate the modulation of such remodeling sites in long-term experiments.

CONCLUSION

The rotational culture system improved chondrocyte plate construction in terms of the production of a homogeneous and abundant ECM that maintained the phenotype of the articular cartilage. The structural properties of the remodeling site were superior to natural healing from an early stage of implantation.

ACKNOWLEDGMENTS

We thank Akira Akatsuka, Yoshiro Shinozaki, and Tomoko Nakai for their expert technical assistance. This work was supported by the Takeda Science Foundation, High-Tech Research Center Project 2004 for Private Universities, and a Grant-in-Aid for Scientific Research from the Ministry of Education, Culture, Sports, Science and Technology and the New Energy and Industrial Technology Development Organization, and Japan Foundation for Aging and Health.

REFERENCES

1. Paget, J. Healing of cartilage. Clin. Orthop. **64,** 7, 1969.
2. Freed, L.E., Martin, I., Vunjak-Novakovic, G. Frontiers in tissue engineering. *In vitro* modulation of chondrogenesis. Clin. Orthop. Relat. Res. **367S,** S46, 1999.
3. Darling, E.M., Athanasiou, K.A. Articular cartilage bioreactor and bioprocess. Tissue Eng. **9,** 9, 2003.
4. Obradovic, B., Martin, I., Padera, R.F., Treppo, S., Freed, L.E., Vunjak-Novakovic, G. Integration of engineered cartilage. J. Orthop. Res. **19,** 1089, 2001.
5. Caplan, A.I., Elyaderani, M., Mocizuki, Y., Wakitani, S., Goldberg, V.M. Principles of cartilage repair and regeneration. Clin. Orthop. Relat. Res. **342,** 254,1997.

6. Solchaga, L.A., Yoo, J.U., Lundberg, M. Dennis, J.E., Huibregtse, B.A., Goldberg, V.M., Caplan, A.I. Hyaluronan-based polymers in the treatment of osteochondral defects. J. Orthop. Res. **18,** 773, 2000.
7. Kaneshiro, N., Sato, M., Ishihara, M., Mitani, G., Sakai, J., Mochida, J. Bioengineered chondrocyte sheets may be potentially useful for the treatment of partial thickness defects of articular cartilage. Biochem. Biophys. Res. Commun. **349,** 723, 2006.
8. Frandal, R.W., Buttle, D.J., Barret, A.J. Improved quantitation and discrimination of sulphated glycosaminoglycans by use of dimethylmethylene blue. Biochim. Biophys. Acta **883,** 173, 1986.
9. Petit, B., Masuda, K., D'souza, A.L., Otten, L., Pietryla, D., Hartmann, D.J., Morris, N.P., Uebelhart, D., Schmid, T.M., Thonar, E.J. Characterization of crosslinked collagens synthesized by mature articular chondrocytes cultured in alginate beads: comparison of two distinct matrix compartments. Exp. Cell. Res. **225,** 151, 1996.
10. Freed, L.E., Hollander, A.P., Martin, I., Barry, J.R., Langer, R., Vunjak-Novakovic, G. Chondrogenesis in a cell-polymer-bioreactor system. Exp. Cell. Res. **240,** 58, 1998.
11. Hayami, T., Funaki, H., Yaoeda, K., Mitui, K., Yamagiwa, H., Tokunaga, K., Hatano, H., Kondo, J., Hiraki, Y., Yamamoto, T., Duong, Le T., Endo, N. Expression of the cartilage derived anti-angiogenic factor chondromodulin-I decreases in the early stage of experimental osteoarthritis. J. Rheumatol. **30,** 2207, 2003.
12. Inoue, T., Osatake, H. A new drying method of biological specimens for scanning electron microscopy. Arch. Histol. Cytol. **51,** 53, 1988.
13. Grogan, S.P., Rieser, F., Winkelmann, V., Berardi, S., Mainil-Varlet, P. A static, closed and scaffold-free bioreactor system that permits chondrogenesis *in vivo*. Osteoarthr. Cartil. **11,** 403, 2003.
14. Hu, J.C., Athanasiou, K.A. A self-assembling process in articular cartilage tissue engineering. Tissue Eng. **12,** 969, 2006.
15. Park, K., Huang, J., Azar, F., Jin, R.L., Min, B.H., Han, D.K., Hasty, K. Scaffold-free, engineered porcine cartilage construct for cartilage defect repair—*in vitro* and *in vivo* study. Artif. Organs **30,** 586, 2006.
16. Furukawa, K.S., Imura, K., Tateishi, T., Ushida, T. Scaffold-free cartilage by rotational culture for tissue engineering. J. Biotechnol. **133,** 134, 2008.
17. Nagai, T., Furukawa, K.S., Sato. M., Ushida. T., Mochida, J. Characteristics of a scaffold-free articular chondrocyte plate grown in rotational culture. Tissue Eng. **14**, 2008, in press.
18. Marlovits, S., Tichy, B., Truppe, M., Gruber, D., Vecsei, V. Chondrogenesis of aged human articular cartilage in a scaffold-free bioreactor. Tissue Eng. **9,** 1215, 2003.
19. Mainil-Varlet, P., Rieser, F., Grogan, S., Mueller, W., Saager, C., Jakob, R.P. Articular cartilage repair using a tissue-engineered cartilage-like implant: an animal study. Osteoarthr. Cartil. **9,** S6, 2001.
20. Brehm, W., Aklin, B., Yamashita, T., Rieser, F., Trub, T., Jakob, R.P., Mainil-Varlet, P. Repair of superficial osteochondral defects with an autologous scaffold-free cartilage construct in a caprine model: implantation method and short-term results, Osteoarthr. Cartil. **14,** 1214, 2006.
21. Martin, I., Obradovic, B., Treppo, S., Grodzinsky, A.J., Langer, R., Freed, L.E., Vunjak-Novakovic, G. Modulation of the mechanical properties of tissue-engineered cartilage. Biorheology **37,** 141, 2000.
22. Schreiber, R.E., Ilten-Kirby, B.M., Dunkelman, N.S., Symons, K.T., Rekettye, L.M., Willoughby, J., Ratcliffe, A. Repair of osteochondral defects with allogeneic tissue engineered cartilage implants, Clin. Orthop. Relat. Res. **367S,** S382, 1999.
23. Shapiro, F., Koide, S., Glimcher, M.J. Cell origin and differentiation in the repair of full-thickness defects of articular cartilage. J. Bone Joint Surg. Am. **75,** 532, 1993.
24. Lee, F.Y-I., Choi, Y.W., Behrens, F.F., DeFouw, D.O., Einhorn, T.A., Programmed removal of chondrocytes during endochondral fracture healing. J. Orthop. Res. **16,** 144, 1998.
25. Gerber, H.P., Vu, T.H., Ryan, A.M., Kowalski, J., Werb, Z., Ferrara, N. VEGF couples hypertrophic cartilage remodeling, ossification and angiogenesis during endochondral bone formation. Nat. Med. **5,** 623, 1999.
26. Hiraki, Y., Inoue, H., Iyama, K., Kamizono, A., Ochiai, M., Shukunami, C., Iijima, S., Suzuki, F., Kondo, J. Identification of chondromodulin I as a novel endothelial cell inhibitor. Purification and its localization in the avascular zone of epiphyseal cartilage. J. Biol. Chem. **272,** 32419, 1997.
27. Kitahara, H., Hayami, T., Tokunaga, K., Endo, N., Funaki, H., Yoshida, Y., Yaoita, E., Yamamoto, T. Chondromodulin-I expression in rat articular cartilage. Arch. Histol. Cytol. **66,** 221, 2003.
28. Gonzalez, A.M., Buscaglia, M., Ong, M., Baird, A. Distribution of basic fibroblast growth factor in the 18-day rat fetus: localization in the basement membranes of diverse tissues. J. Cell. Biol. **110,** 753, 1990.
29. Gelb, D.E., Rosier, R.N., Puzas, J.E. The production of transforming growth factor-beta by chick growth plate chondrocytes in short term monolayer culture. Endocrinology **127,** 1941, 1990.
30. Thiennu, H.V., Shipley, J.M., Bergers, G., Burger, J.E., Helms, J.A., Hanahan, D., Shapiro, S.D., Senior, R.M., Werb, Z. MMP-9/Gelatinase B is a key regulator of growth plate angiogenesis and apoptosis. Cell **93,** 411, 1998.

Address reprint requests to:
Masato Sato, M.D., Ph.D.
Department of Orthropaedic Surgery, Surgical Science
Tokai University School of Medicine
143 Shimokasuya
Isehara, Kanagawa 259–1193
Japan

E-mail: sato-m@is.icc.u-tokai.ac.jp

Received: July 24, 2007
Accepted: January 18, 2008